Available online at www.sciencedirect.com
SCIENCE DIRECT
Trans. Nonferrous Met. Soc. China 16(2006) 917−921
Transactions of Nonferrous Metals Society of China
www.csu.edu.cn/ysxb/

Effect of pre-aging on precipitation behavior of Al-1.29Mg-1.22Si-0.68Cu-0.69Mn-0.3Fe-0.2Zn-0.1Ti alloy

LIU Hong(刘 宏)[1], CHEN Yang(陈 扬)[2], ZHAO Gang(赵 刚)[3],
LIU Chun-ming(刘春明)[3], ZUO Liang(左 良)[3]

1. School of Mechanical Engineering, Shandong Institute of Light Industry, Ji'nan 250100, China;
2. College of Material and Chemical Engineering, Liaoning Institute of Technology, Jinzhou 121001, China;
3. School of Materials and Metallurgy, Northeastern University, Shenyang 110004, China

Received 16 February 2006; accepted 26 April 2006

Abstract: By means of Vickers-hardness and electrical conductivity measurements, DSC tests and TEM analyses, the effect of different pre-aging treatments on precipitation characteristic of the Al-1.29Mg-1.22Si-0.68Cu-0.69Mn-0.3Fe-0.2Fe-0.1Ti (mass fraction, %) alloy during subsequent artificial aging was investigated. The results indicate that with increasing pre-aging time from 2.5 min to 10 min at 170 ℃, the number of formed β'' nuclei increases, resulting in promoting artificial aging kinetics and enhancing peak hardness. The hardness of pre-aged alloy reduces within lower temperature range of non-isothermal aging and increases in early stage of isothermal aging at 170 ℃. The size and density of clusters in pre-aged samples determine the hardenability in early stage of artificial aging. Pre-aging has dual mechanisms: namely, clusters (β'' nuclei) formed by pre-aging can inhibit the precipitation of GP zones during natural aging, and can quicken the precipitation of β'' phase in the early stage of subsequent artificial aging.

Key words: aluminum alloys; pre-aging; non-isothermal aging; isothermal aging; β'' nucleus

1 Introduction

Aluminum alloys of the 6000 series, containing Mg and Si as the major solutes, are strengthened by the precipitation of metastable precursors of the equilibrium $\beta(Mg_2Si)$ phase. The precipitation of these metastable precursors occurs in one or more sequences, which is quite complex and not fully understood due to different compositions of alloys[1−4]. This largely causes confusions regarding the number of precipitation sequences, involving number, structure and composition of the metastable precursors[5−8] during aging. However, the variation of pre-aging on this precipitation process, especially, the effect of pre-aging on metastable precursors produced in subsequent artificial aging is more important in strengthening of alloys[9−12]. But the investigation on this aspect is not systematic up to now.

In this study the authors investigated the effect of different pre-aging treatments on the precipitation characteristic during subsequent artificial aging of Al-1.29Mg-1.22Si-0.68Cu-0.69Mn-0.3Fe-0.2Zn-0.1Ti(mass fraction, %) alloy. It has quite great significance for 6000 series aluminum alloys for automobile body sheets application to gain baking strengthening.

2 Experimental

The alloy studied in this work was prepared using high purity aluminium (99.9%), electrolysis copper, industrial pure magnesium and zinc, and intermediate alloys of Al-9.5Si, Al-9.0Mn and Al-3Ti (mass fraction, %). These raw materials were melted in a resistance crucible oven as per a certain adding order, and then cast into ingots (220 mm×120 mm×30 mm) in the copper mould with cooling water. The chemical composition of the alloy prepared is Al-1.29Mg-1.22Si- 0.68Cu-0.69Mn-0.3Fe-0.2Zn-0.1Ti (mass fraction, %). Two-stage homogenization treatments of the ingots were performed at 470 ℃ for 5 h and at 540 ℃ for 16 h. Then the ingots were hot-rolled and cold-rolled to thin sheets of 1.2 mm thickness.

Foundation item: Project(2002AA331050) supported by The Hi-tech Research and Development Program of China; Project(0208) supported by the Science and Technology Research of Ministry of Education of China
Corresponding author: LIU Hong; Tel: +86-531-88523981; E-mail: hongshuoxin@163.com

All the samples used in this experiment were taken from cold-rolled thin sheets. The size of samples for hardness and electrical conductivity measurements was 20 mm×20 mm. The samples for the DSC analyses are disc of 6 mm in diameter and 0.5 mm in thickness. The samples for TEM observation were ground to a thickness of 0.06 mm and twin jet electropolished in a solution of 30% HNO_3 (volume fraction) and 70% CH_3OH at −25 ℃ to −20 ℃.

All the samples were solution treated at 540 ℃ for 30 min, and immediately aged at 170 ℃ for 2.5−10 min, and subsequently naturally aged for two weeks (T4P temper). Then the samples after T4P temper were non-isothermally aged, namely the samples were heated to the corresponding temperatures on the DSC traces at the same heating rate of DSC tests and kept for 1 min before quenching to room temperature, or isothermally aged at 170 ℃ for different times respectively. The samples after the above treatments were measured for hardness and electrical conductivity and analyzed through combining the measured results with the DSC and TEM results.

DSC analysis of the samples was performed in a Setaram−DSC131. During the DSC measurement, the samples were heated at 10 ℃/min and protected with flowing argon. A high purity aluminium crucible with the same mass of the samples was used as reference. A 450SVD Wilson hardness tester was used for hardness measurements. The electrical conductivity was measured with SMP10 conductivity meter. The TEM observation was carried out using a Tecnaz transmission electron microscope operated at 200 kV.

3 Experimental results

3.1 DSC analysis

Fig.1 shows the DSC traces of the alloy after T4P treatments for different times. Two exothermic peaks can be clearly seen in the DSC traces. Correlated with the results of other researchers[10−13], it is reasonable to believe that the precipitations corresponding to these two peaks are β'' and β' phases respectively, but there is no GP zone peak in the DSC traces. With the increasing of pre-aging time, β'' exothermic peak gets more flat and the temperature of β'' peak decreases.

Further DSC experiments were conducted after isothermal aging at 170 ℃ for 30 min in T4P (5 min) and T4P (7.5 min) tempers, as shown in Figs.2(a) and (b) respectively. It is obvious that the longer the pre-aging time is, the lower the β'' peak in DSC traces is.

3.2 Aging behavior

Fig.3 shows the hardness and electrical conductivity curves corresponding to the DSC traces of samples after non-isothermal aging in T4P (2.5 min), T4P (5 min) and T4P (10 min) tempers, respectively. Within lower temperature range of non-isothermal aging there is a hardness trough in the DSC trace and the trough shifts to lower temperature with increasing pre-aging time, but the peak hardness of β'' peak rises. The variation rule of

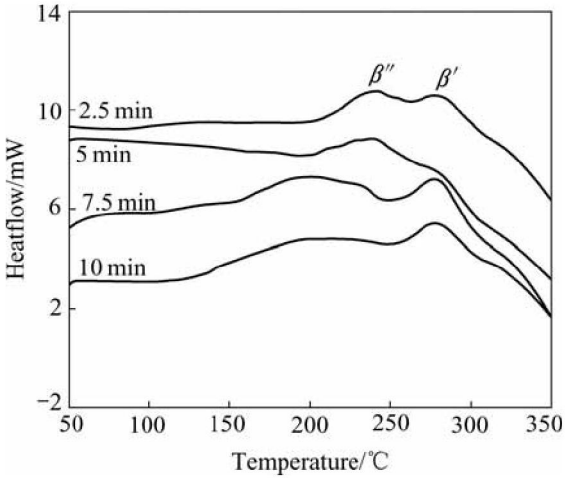

Fig.1 DSC traces of alloy after T4P treatments for different times

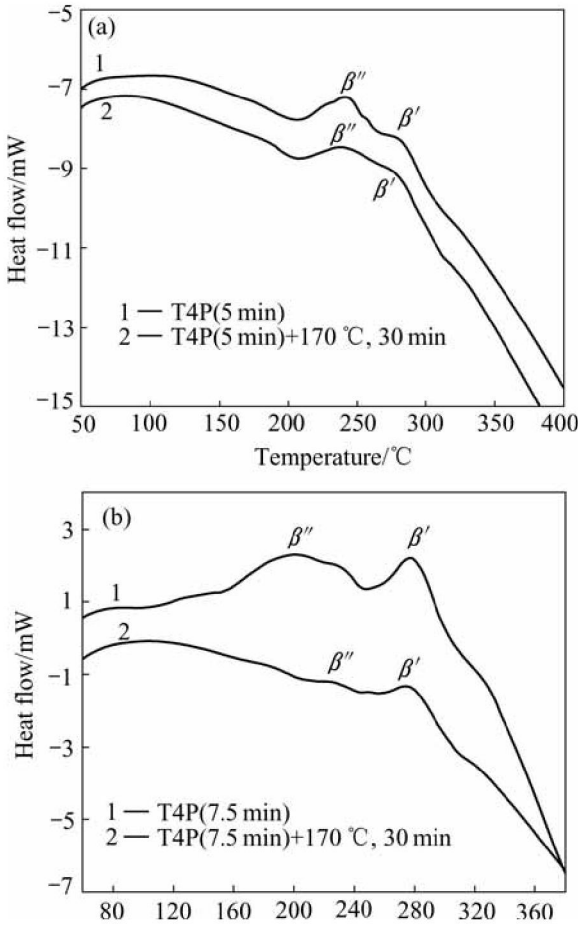

Fig.2 DSC traces of alloy after isothermal aging at 170 ℃ for 30 min in T4P (5 min)(a) and T4P (7.5 min)(b) tempers

electrical conductivity is essentially the same, namely, the electrical conductivity peak corresponds to the hardness trough.

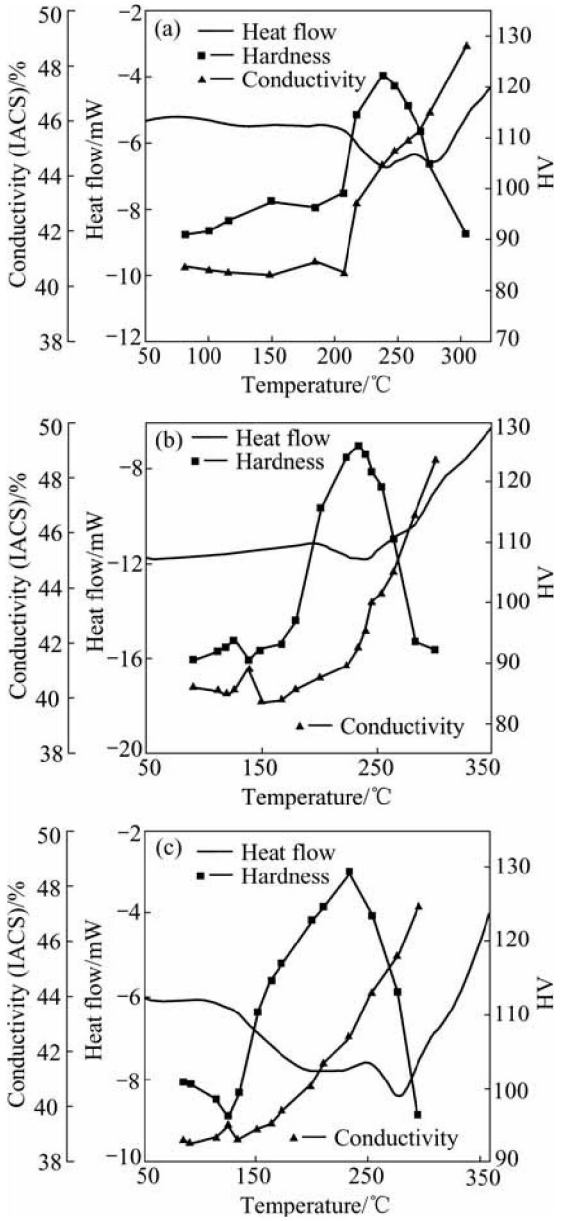

Fig.3 Hardness and electrical conductivity curves corresponding to DSC traces of alloy after non-isothermal aging in T4P (2.5 min)(a), T4P (5 min)(b) and T4P (10 min)(c) tempers

Fig.4 gives the variation curves of hardness and electrical conductivity of alloy isothermally aged at 170 ℃ after T4P treatments for different times. It is obvious from Fig.4(a) that the alloy doesn't show any hardness reduction in the early stage of aging, and increasing pre-aging time not only quickens the rate of aging kinetics in the early stage of artificial aging but also enhances the peak hardness. It can be seen from Fig.4(b) that the variation trend of all the electrical conductivities are basically similar, the difference in the early stage of aging is that the degree of electrical conductivity reduction abates with the increment of pre-aging time.

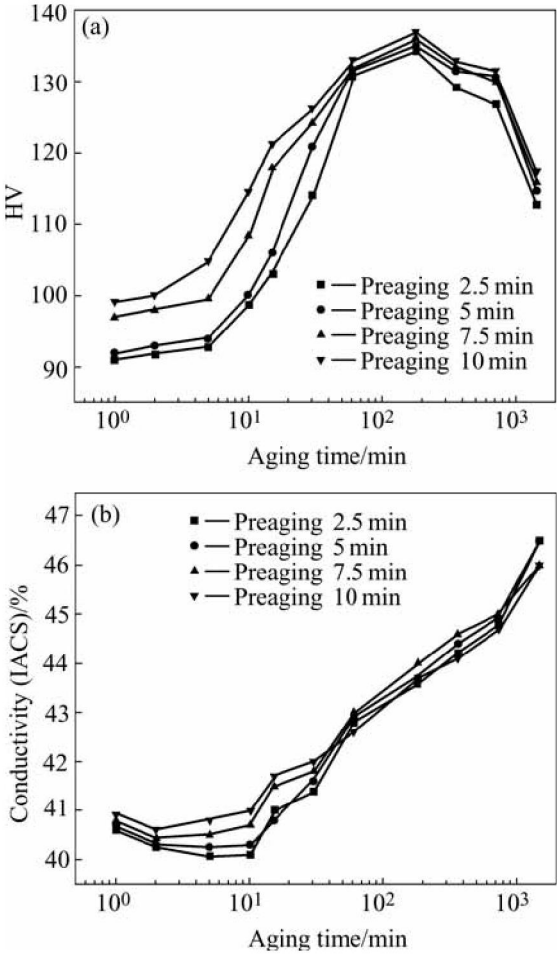

Fig.4 Effects of T4P treatments for different times on hardness (a) and electrical conductivity (b) of alloy isothermally aged at 170 ℃

3.3 TEM observation

The TEM bright field images of the alloy after different tempers are shown in Fig.5. In pre-aging at 170 ℃ for 5 min temper, there is no any evident precipitation characteristic in the matrix (as shown in Fig.5(a), where the phase marked by arrow is dispersed phase); after isothermally aged at 170 ℃ for 10 min, the dimly visible β'' precipitates appear but the number is small (the phase marked by arrow in Fig.5(b)); after aged for 30 min, the number of β'' precipitates increases markedly (the phase marked by arrow in Fig.5(c)), and distributes evenly. The larger size precipitates in Figs.5(b) and (c) are β'' phase distributed at grain boundaries.

4 Discussion

The effect of pre-aging on precipitation behavior of subsequent aging is demonstrated quite convincingly by the DSC experiments performed in the T4P tempers. The disappearance of the GP zone peak and the presence of

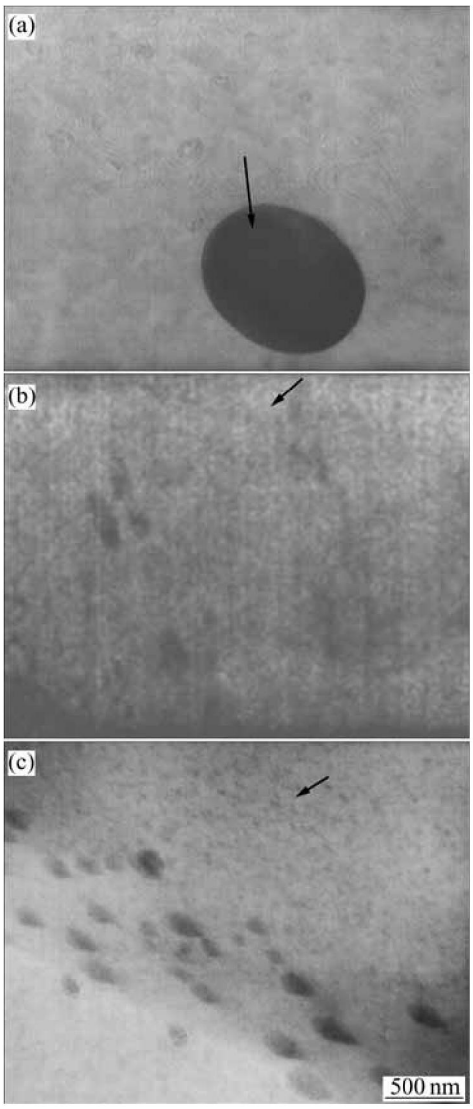

Fig.5 TEM bright field micrographs of alloy after different tempers: (a) T4P(5 min) temper; (b) Isothermally aged at 170 ℃ for 10 min; (c) Isothermally aged at 170 ℃ for 30 min

β'' peak in the DSC traces (Fig.1) indicate that GP zones (or β'' nuclei) instead of β'' phase exist in the pre-aged samples. No appearance of endothermic peak in front of β'' peak suggests that the formation of GP zones during natural aging is effectively restrained.

However, the evidence of a little drop of hardness within lower temperature range of non-isothermal aging (Fig.3) indicates that clustering activities still proceed during natural aging following pre-aging at this temperature. The electrical conductivity peak corresponding to hardness trough reveals that the formed GP zones dissolve during the non-isothermal aging. The precipitation of GP zones decreases with the increment of pre-aging time, which is just in accordance with the experimental phenomenon of decrescent trend of hardness trough. This shows that the less the number of dissolved GP zones is during DSC heating, the more effective the pre-aging is for suppressing their formation. The precipitation kinetics of β'' phase rests with the sizes and density of clusters in the pre-aged microstructures [14, 15], which can be proved by the shift of β'' peak to lower temperature and increment of β'' peak hardness with increasing pre-aging time.

No hardness drop during isothermal aging at 170 ℃ (Fig.4(a)) is because the degree of hardness enhancement caused by the growth of β'' nuclei is more than the degree of hardness reduction caused by the dissolution of GP zones. In early stage of aging, the extent of electrical conductivity drop abates with the increment of pre-aging time (Fig.4(b)), which provides the evidence for increased β'' nuclei produced by pre-aging to make clustering process of natural aging slower, and the fact that β'' peak in the DSC trace lessens after isothermal aging at 170 ℃ (Fig.2) just reflects the increase of number of β'' phase in artificially aged microstructures. The larger the number of β'' nucleus formed by pre-aging is, and the larger their sizes are, the more easily they develop into β'' phase during artificial aging. This guess just accords with the experimental results of quickening of β'' precipitation and increasing of peak hardness shown in Fig.4(a).

Moreover，further evidence of β'' nuclei formed by pre-aging is from TEM micrographs (Fig.5). The precipitation in the T4P (5 min) temper sample does not show any distinguished features. But the sparse β'' phase produced by isothermal aging at 170 ℃ for 10 min, and the appearance of large number of β'' phase whose edge is clear for 30 min, can indirectly prove that pre-aging forms β'' nuclei which continuously develop into β'' phase during isothermal aging at 170 ℃.

According to the above analyses, the size and density of clusters in pre-aged microstructures determine the hardenability in the early stage of artificial aging. The precipitation of GP zones during natural aging can be effectively restrained when pre-aging forms enough and stable β'' nuclei, and consequently softening of alloy can be avoided in the early stage of artificial aging. This is vital currently for the condition of most interest to the automotive baking finish (to be equivalent to aging at 170 ℃ for 30 min). The effects of pre-aging on subsequent artificial aging are that clusters (β'' nuclei) produced by pre-aging slower the process of natural aging, and that these nuclei accelerate the precipitation of β'' phase during subsequent artificial aging.

5 Conclusions

1) Prolonging pre-aging time from 2.5 min to 10 min at 170 ℃, the number of formed β'' nuclei increases, resulting in quickening subsequent artificial aging kinetics and enhancing peak hardness.

2) The hardness of alloy pre-aged at 170 ℃ within 2.5−10 min reduces in lower temperature range of non-isothermal aging and increases in the early stage of isothermal aging at 170 ℃.

3) The size and density of clusters in pre-aged samples determines the hardenability in the early stage of artificial aging. Pre-aging has dual mechanisms: one is that clusters (β'' nuclei) formed by pre-aging can inhibit the precipitation of GP zones during naturally aging before artificial aging; the other is that these β'' nuclei can quicken precipitation of β'' phase in the early stage of subsequent artificial aging and consequently can promote the aging hardening.

References

[1] EDWARDS G A, STILLER K, DUNLOP G L, COUPER M J. The precipitation sequence in Al-Mg-Si alloys [J]. Acta Mater, 1998, 46(11): 3893−3904.

[2] MURUYAMA N, UEMORI R, HASHIMOTO N. Effect of silicon addition on the composition and structure of fine-scale precipitation in Al-Mg-Si alloys [J]. Scripta Mater, 1997, 36(1): 89−93.

[3] GUPA A K, LLOYD D J, COURT S A. Precipitation hardening in Al-Mg-Si alloys with and without excess Si [J]. Mater Sci Eng A, 2001, 316(1−2): 11−17.

[4] MURAYAMA M, HONO K. Pre-precipitate clusters and precipitation processes in Al-Mg-Si alloys [J]. Acta Mater, 1999, 47(1): 1537−1548.

[5] GUPTA A K, LLOYD K J, COURT S A. Precipitation hardening processes in Al-0.4%Mg-1.3%Si-0.25%Fe aluminum alloy [J]. Mater Sci Eng A, 2001, 301(2): 140−146.

[6] PEROVIC A, PEROVIC D D, WEATHERLY G C, LIOYD D J. Precipitation in aluminum alloys AA6111 and AA6016 [J]. Scripta Mater, 1999, 41(7): 703−708.

[7] MIAO W F, LAUGHLIN D E. Precipitation hardening in aluminum alloy 6022 [J]. Scripta Mater, 1999, 40(7): 873−878.

[8] ZHEN L, KANG S B. Effect of natural aging and preaging on subsequent precipitation process of Al-Mg-Si alloys with high excess silicon [J]. Materials Science and Technology, 1997, 13 (11): 905−910.

[9] MIAO W F, LAUGHLIN D E. Effects of Cu content and preaging on precipitation characteristics in aluminum alloy 6022 [J]. Metall Mater Trans A, 2000, 31(2): 361−371.

[10] BRYANT J D. The effects of preaging treatments on aging kinetics and mechanical properties in AA6111 aluminum autobody sheet [J]. Metall Mater Trans A, 1999, 30(10): 1999−2006.

[11] MIAO W F, LAUGHLIN D E. A differential scaning calorimetry study of aluminum alloy 6111 with different pre-aging treatments [J]. J Mater Sci Lett, 2000, 19(2): 201−203.

[12] YAO J Y, GRAHAM D A, RINDERER B, COUPER M J. A TEM study of precipitation in Al-Mg-Si alloys [J]. Micron, 2001, 32(8): 865−870.

[13] ZHEN L, KANG S B. DSC analyses of the precipitation behavior of two Al-Mg-Si alloys naturally aged for different times [J]. Materials Letters, 1998, 37(2): 349−453.

[14] ESMAELI S, LLOYD D J, POOLE W J. Effect of natural aging on the resistivity evolution during artificial aging of the aluminum alloy AA6111 [J]. Materials Letters, 2005, 59(3): 575−577.

[15] KLEINER S, HENKEL CH, SCHULZ P, RANSHOFEN, UGGOWITZER P J. Paint bake response of aluminium alloy 6016 [J]. Aluminium, 2001, 77(3): 185−189.

(Edited by YUAN Sai-qian)